

## Electronic Structures and Magnetism of the MgCFe<sub>3</sub>(001) Surface

Ying Jiu Jin, I. G. Kim and J. I. Lee\*

Department of Physics, Inha University, Incheon 402-751, Korea

(Received 12 June 2002)

The electronic structures and magnetism of the non-oxide perovskite MgCFe<sub>3</sub>(001) surface were investigated by using the all-electron full-potential linearized augmented plane wave (FLAPW) method within the generalized gradient approximation (GGA). We considered both of the MgFe terminated (MgFe-Term) and the CFe terminated (CFe-Term) surfaces. We found that the minority spin *d*-bands of Fe(S) of the MgFe-Term are strongly localized and Fermi level ( $E_F$ ) lies just below the sharp peak of the minority spin *d*-band of Fe(S), while the minority spin *d*-bands of Fe(S) of the CFe-Term are not localized much and Fermi level ( $E_F$ ) lies in the middle of two peaks of the minority spins. The majority Fe(S) *d*-band width of MgFe-Term is narrower than that of the CFe-Term. It is found that the magnetic moment of Fe(S) of the MgFe-Term is 2.51  $\mu_B$ , which is much larger than that of 1.97  $\mu_B$  of the CFe-Term.

**Key words :** First-principles calculation, Surface magnetism, Surface electronic structure, MgCFe<sub>3</sub>

### 1. Introduction

The recent discovery of superconductivity of the nickel rich non-oxide perovskite MgCNi<sub>3</sub> [1] has attracted much attention. MgCNi<sub>3</sub> has superconducting transition temperature,  $T_c \sim 8$  K, with cubic perovskite structure: Mg atom at (0 0 0), C atom at (1/2 1/2 1/2), and Ni atoms at (1/2 1/2 0), (1/2 0 1/2), and (0 1/2 1/2). The effects of various doping to the electronic structures of intrinsic MgCNi<sub>3</sub>, and consequently to its superconductivity and magnetism, have been investigated by many authors [2-6]. Shim *et al.* [2, 3] investigated the effect of doping of C site by B or N atoms and that of Mg site by Li or Al atoms. Rosner *et al.* [4] also investigated the effect of doping of Mg site by Li or Na atoms. Szajek [5] found that the small concentrations of impurity of hole-Co or electron-Cu doping do not lead to magnetic order by using the self-consistent tight-binding linear muffin-tin orbital (TB-LMTO) method. However, with increasing the number of *d*-band hole by doping Co or Fe on the Ni-site [6], the MgCNi<sub>3</sub> becomes paramagnetic and then ferromagnetic. The MgCNi<sub>3-x</sub>Co<sub>x</sub> occurs ferromagnetic transition for  $x = 2$ , but the MgCNi<sub>3-x</sub>Fe<sub>x</sub> become ferromagnetic before  $x = 2$ . According to the first-principles calculation by using the all-electron full-potential linearized augmented plane wave (FLAPW)

method within generalized gradient approximation (GGA), the magnetic moment of Fe is 1.42  $\mu_B$  for bulk MgCFe<sub>3</sub> [6].

The reduced symmetry and the lower coordination numbers at surface lead to novel features on its electronic structures. For example, Kim *et al.* [7] investigated the surface electronic structures of MgCNi<sub>3</sub>(001). They found that the number of *d* electrons of Ni of the MgNi terminated surface is more than that of the CNi terminated surface. This fact is due to the strong hybridization between the C-*p* and Ni-*d* states. They also calculated that the work function of the MgNi terminated surface is lower than that of the CNi terminated surface. No magnetic ordering was found for the both terminations of the MgCNi<sub>3</sub>(001) surfaces.

In this paper, we have calculated the electronic structure of MgCFe<sub>3</sub>(001) both for the MgFe terminated (MgFe-Term) and the CFe terminated (CFe-Term) surfaces, and their surface magnetism by using the all-electron FLAPW method within the generalized gradient approximation (GGA). We briefly describe the calculational methods in Sec. II and present the results and discussions in Sec. III. A brief summary is given in Sec. IV.

### 2. Calculational Methods

In order to compare the effects of the different atomic terminations on the electronic structures and magnetism

\*Corresponding author: Tel: +82-32-860-7654, e-mail: jilee@inha.ac.kr

of the  $\text{MgCFe}_3(001)$  surfaces, we considered two systems consisted of the MgFe terminated (MgFe-Term) and the CFe terminated (CFe-Term) surfaces. Each system is made of a nine-layer single slab along the [001] direction of the perovskite  $\text{MgCFe}_3$ . The two dimensional (2D) lattice constant was chosen to be 7.20 a.u., which is the experimental lattice constant of  $\text{MgCNi}_3$  [1], and the interlayer distances were chosen to be 3.60 a.u., half of the lattice constant. Neither surface relaxations nor reconstructions were considered.

The Kohn-Sham equation was solved self-consistently in terms of the all-electron FLAPW method [8] within the GGA [9]. The integrations over the 2D Brillouin zone (BZ) were performed by summations over 21  $\mathbf{k}$ -points inside the  $1/8$  wedge of the irreducible 2D-BZ. The wave functions were expanded with  $\sim 1600$  linearized augmented plane waves (LAPWs) per each  $\mathbf{k}$ -point and spin. The wave functions, the charge densities, and the potential were expanded with  $l \leq 8$  lattice harmonics inside each muffin-tin (MT) sphere with the radii of 2.50, 2.30, and 1.20 a.u. for the Mg, Fe, and C atoms, respec-

tively. All core electrons were treated fully relativistically, while valence states were treated scalar relativistically, without considering spin-orbit coupling [10]. Self-consistency was assumed when the root-mean-square distances between the input and output total charges and spin densities are less than  $1.0 \times 10^{-4}$  electrons/a.u.<sup>3</sup>

### 3. Results and Discussions

The contour plots of total charge density of (a) the MgFe-Term in (110) plane and (b) the CFe-Term in (200) plane are presented in Fig. 1. The lowest contour starts from  $1.0 \times 10^{-3}$  electrons/a.u.<sup>3</sup> and increase successively by a factor of  $\sqrt{2}$ . A strong covalent-like Fe-C bonding along the interstitial region between the Fe and C atoms is found by the strong charge accumulations in the interstitial region. The charge density profiles between the Fe and C atoms were extended a little along the direction of Fe-C. From Fig. 1, we also found that the charge densities are similar to each other for the inner layers, that is the S-2, S-3, and the center layers. In the vacuum

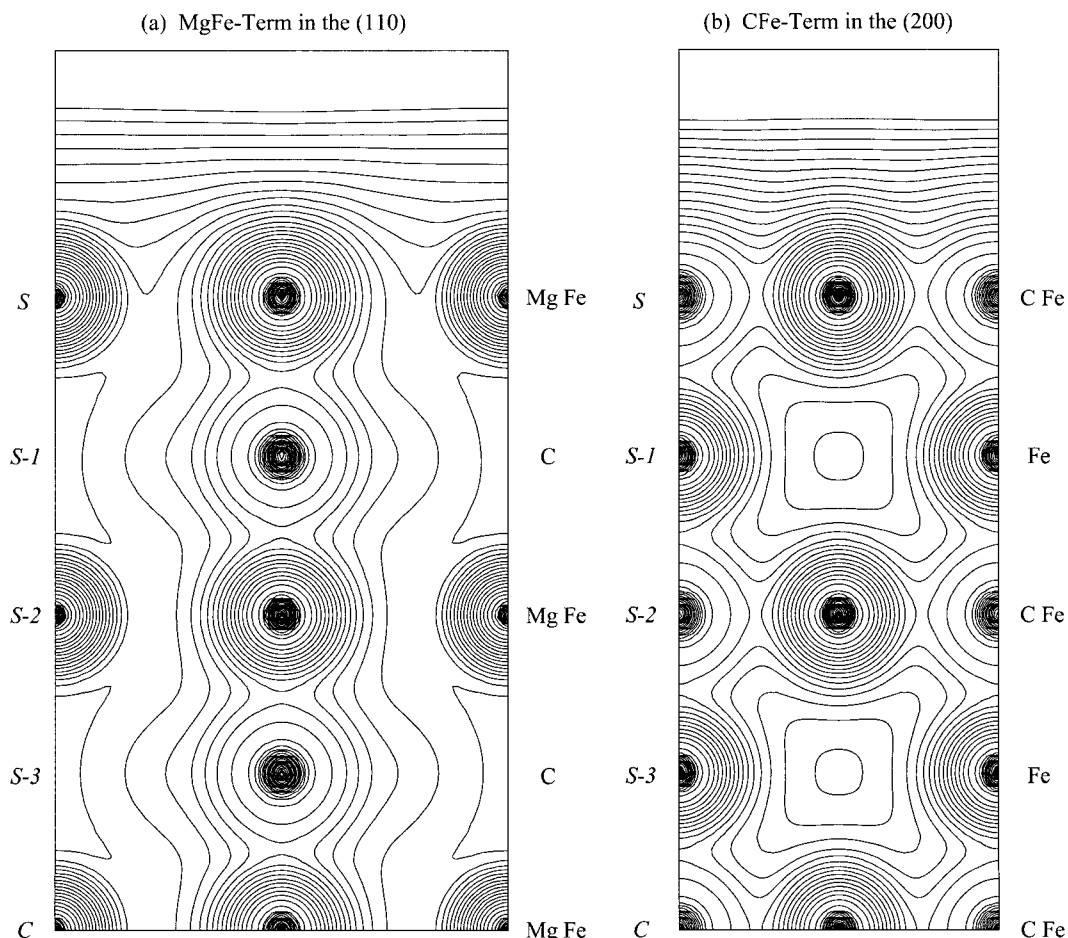


**Fig. 1.** The total charge density contour plots of (a) the MgFe-Term in the (110) plane and (b) the CFe-Term in the (200) plane, for the  $\text{MgCFe}_3(001)$  surfaces. Contour starts from  $1.0 \times 10^{-3}$  electrons/a.u.<sup>3</sup> and increase successively by a factor of  $\sqrt{2}$ .

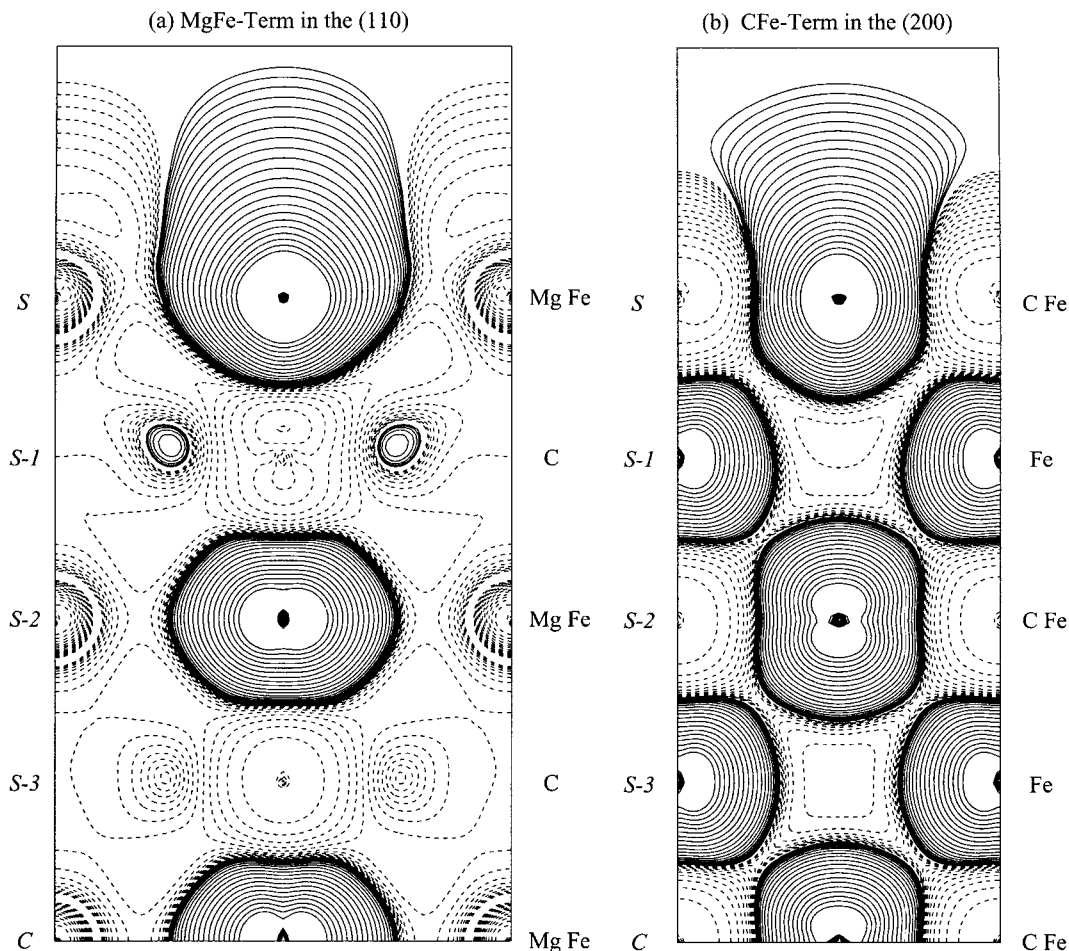


**Fig. 2.** The spin density contour plots of (a) the MgFe-Term in the (110) plane and (b) the CFe-Term in the (200) plane, for the MgCFe<sub>3</sub>(001) surfaces. The solid and broken lines represent the positive and the negative spins, respectively.

region, the density profile of the CFe-Term has rather steep gradient, while that of the MgFe-Term is extended little far away from the surface. These “spilled-out” charges lead to the formation of the dipole barrier, which determines the work function. The calculated work function of the MgFe-Term is 4.10 eV, while that of the CFe-Term is 4.73 eV.

The spin density contour plots of (a) the MgFe-Term in the (110) plane and (b) the CFe-Term in the (200) plane are presented in Fig. 2. The solid and dashed lines represent the positively and the negatively polarized spins, respectively. The lowest contour start from  $1.0 \times 10^{-4}$  electrons/a.u.<sup>3</sup> and increase successively by a factor of  $\sqrt{2}$ . It is found that the spin-up *d*-electrons are localized around the Fe sites. Contrastingly, the interstitial region and the vicinity of the C and Mg sites have negative polarizations, except in the *S*-1 layer of the MgFe-Term. There are small positive regions in the vicinity of the C atomic sites at the *S*-1 layer of the MgFe-Term. It is interesting to find that the positive spin density around

Fe-site is oriented with the axis toward the neighboring C-site in the both terminations.

Concentrating on the surface region, the spin density profile of Fe(*S*) of the MgFe-Term is erupted more than that of the CFe-Term. This fact implies a large difference in the magnetic moments of the surface Fe atoms between the MgFe-Term and the CFe-Term. The calculated layer-by-layer magnetic moments of the Fe atoms are tabulated in Table 1. The magnetic moment of Fe(*S*) of the MgFe-Term is 2.51  $\mu_B$ , which is much larger than that of 1.97  $\mu_B$  of the CFe-Term. Away from the surfaces, the magnetic

**Table 1.** The layer-by-layer magnetic moments of Fe atoms (in units of  $\mu_B$ ) inside each MT sphere.

Atom	the MgFe-Term	the CFe-Term
Fe( <i>S</i> )	2.51	1.97
Fe( <i>S</i> -1)	1.44	1.56
Fe( <i>S</i> -2)	1.54	1.44
Fe( <i>S</i> -3)	1.41	1.52
Fe( <i>C</i> )	1.45	1.44

**Table 2.** Number of layer-projected  $l$ -decomposed spin up ( $\uparrow$ ) and spin down ( $\downarrow$ ) valence charges inside each MT spheres.

MgFe-Term											
		$s$	$p$	$d$	total			$s$	$p$	$d$	total
Fe(S)	$\uparrow$	0.18	0.15	4.32	6.83	Mg(S)	$\uparrow$	0.21	0.18	0.05	0.98
	$\downarrow$	0.16	0.14	1.84			$\downarrow$	0.25	0.23	0.05	
Fe(S-1)	$\uparrow$	0.18	0.23	3.85	7.14	C(S-1)	$\uparrow$	0.27	0.43	0.01	1.47
	$\downarrow$	0.18	0.24	2.40			$\downarrow$	0.28	0.49	0.01	
Fe(S-2)	$\uparrow$	0.18	0.22	3.90	7.12	Mg(S-2)	$\uparrow$	0.21	0.22	0.07	1.15
	$\downarrow$	0.18	0.24	2.34			$\downarrow$	0.24	0.28	0.08	
Fe(S-3)	$\uparrow$	0.18	0.22	3.84	7.13	C(S-3)	$\uparrow$	0.27	0.43	0.01	1.47
	$\downarrow$	0.18	0.24	2.41			$\downarrow$	0.28	0.49	0.01	
Fe(C)	$\uparrow$	0.18	0.22	3.86	7.13	Mg(C)	$\uparrow$	0.21	0.22	0.07	1.15
	$\downarrow$	0.18	0.24	2.39			$\downarrow$	0.24	0.28	0.08	
CFe-Term											
		$s$	$p$	$d$	total			$s$	$p$	$d$	total
Fe(S)	$\uparrow$	0.19	0.20	4.06	6.99	C(S)	$\uparrow$	0.27	0.41	0.00	1.45
	$\downarrow$	0.17	0.21	2.10			$\downarrow$	0.28	0.49	0.00	
Fe(S-1)	$\uparrow$	0.18	0.22	3.92	7.14	Mg(S-1)	$\uparrow$	0.21	0.22	0.07	1.14
	$\downarrow$	0.18	0.24	2.33			$\downarrow$	0.24	0.29	0.08	
Fe(S-2)	$\uparrow$	0.18	0.22	3.85	7.14	C(S-2)	$\uparrow$	0.27	0.43	0.01	1.47
	$\downarrow$	0.18	0.24	2.40			$\downarrow$	0.28	0.49	0.01	
Fe(S-3)	$\uparrow$	0.18	0.22	3.89	7.13	Mg(S-3)	$\uparrow$	0.21	0.22	0.07	1.15
	$\downarrow$	0.18	0.24	2.36			$\downarrow$	0.24	0.28	0.08	
Fe(C)	$\uparrow$	0.18	0.22	3.85	7.14	C(C)	$\uparrow$	0.27	0.43	0.01	1.47
	$\downarrow$	0.18	0.24	2.39			$\downarrow$	0.28	0.49	0.01	

moment of Fe converges quickly to the value of  $1.44 \mu_B$  of Fe(C) in the both terminations. The magnetic moments of Fe(C) of the both terminations are close to the bulk value of  $1.42 \mu_B$  [6].

The calculated numbers of the  $l$ -decomposed spin-polarized electrons inside the MT spheres for the both systems are given in Table 2. We found that the number of the  $s$ -electrons of each atom is almost constant in all the layers. Such feature is also seen for the case of the  $p$ -electrons except for the surface layers, where both the majority and minority spin  $p$ -electrons were decreased compared to those of the center layers. The numbers of the majority (minority) spin  $p$ -electrons of the surface layer of the MgFe-Term is decreased by 0.07 (0.10) for Fe(S) and 0.04 (0.05) for Mg(S), with respect to that of the center layer. But the decrements of the majority (minority) spin  $p$ -electrons of the surface layer of the CFe-Term are much smaller, only 0.02 (0.03) for Fe(S) and 0.02 (0.00) for C(S).

The number of the majority spin  $d$ -electrons of Fe(S) of the MgFe-Term is increased about 0.46, while the minority spin  $d$ -electrons of Fe(S) of the MgFe-Term is decreased about 0.55, with respect to those of Fe(C). In the CFe-

Term, the majority spin  $d$ -electrons of Fe(S) is increased by 0.21, while the number of the minority spin  $d$ -electrons of Fe(S) is decreased by 0.29. Those values of the increment or decrement in the MgFe-Term are much larger than those in the CFe-Term. This fact is consistent with the one that the value of magnetic moment of Fe(S) of the MgFe-Term is larger than that of the CFe-Term. It is found that the numbers of the total electrons of the Fe atoms in the both terminations have almost constant value of 7.14 in all the layers except at the surfaces, where the numbers of the total electrons of Fe(S) of the MgFe-Term and the CFe-Term are decreased to 6.83 and 6.99, respectively.

The layer-projected spin-polarized density of states (DOS) of (a) the MgFe-Term and (b) the CFe-Term of MgFe<sub>3</sub>(100) inside each MT sphere is presented in Fig. 3. Fermi level ( $E_F$ ) is set to zero. Solid lines represent the total DOS of the Fe atoms, while the broken lines represent the total DOS of the Mg or C atoms with the magnification factor of 10. The minority spins are factored by -1. It is interesting to find that  $E_F$  of the MgFe-Term lies just below the sharp peak of the surface state of the minority spin DOS, while that of the CFe-Term lies in the

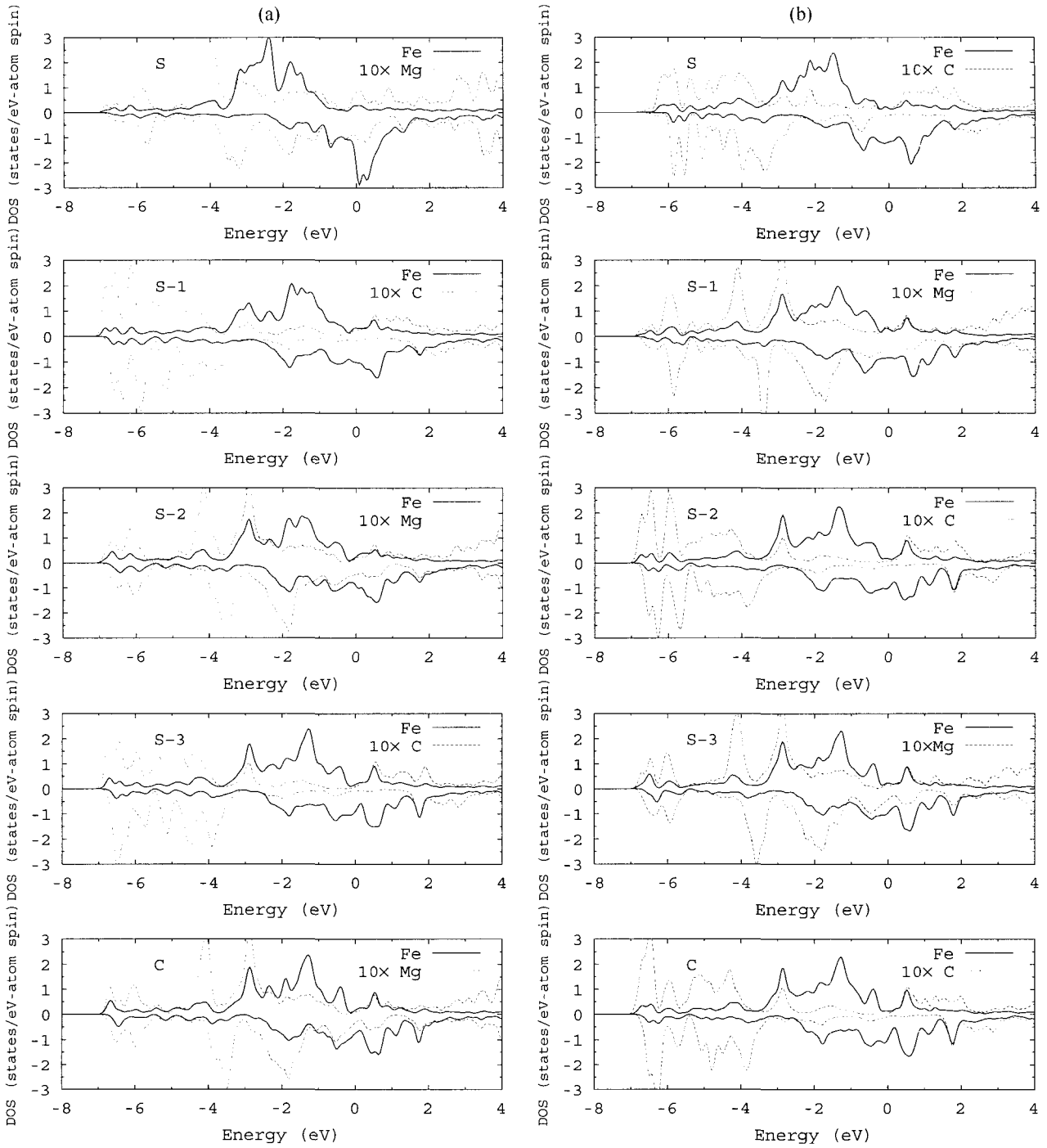


**Fig. 3.** The layer-projected spin-polarized density of states (LDOS) of (a) the MgFe-Term and (b) the CFe-Term of  $\text{MgCFe}_3(100)$ . Fermi level is set to zero.

middle of the two peaks of the minority spin DOS. This feature is due to the strong hybridizations between the  $\text{Fe}(S)\text{-}d$  states and the  $\text{C}(S)\text{-}p$  states in the CFe-Term. Such strong hybridizations are also found in the  $\text{MgCNi}_3(001)$  surfaces [7]. For the minority spin  $p$ -states of  $\text{C}(S)$  of the CFe-Term, a new peak is appeared at  $\sim -0.7$  eV, which is strongly hybridized with the minority spin  $\text{Fe}(S)\text{-}$

$d$  states.

We also find an interesting feature that the majority  $d$ -band widths of  $\text{Fe}(S)$  in both the terminations are narrowed much. The two peaks of the majority spin  $\text{Fe}\text{-}d$  states at  $\sim -0.4$  eV and at  $\sim 0.5$  eV are gradually reduced as we go to the surface layer from the center layer in the CFe-Term, while the peaks almost disappear in the MgFe-

Term. Most of the majority  $d$ -bands of Fe( $S$ ) of the MgFe-Term are located in the range between -3.5 and -1.0 eV, and most of the majority  $d$ -bands Fe( $S$ ) of the CFe-Term are located between -3.5 and -0.5 eV. Interestingly, the peak position of the majority  $d$ -bands of Fe( $S$ ) of the MgFe-Term at  $\sim$ -3.2 eV is shifted by  $\sim$ 0.3 eV to lower energy than that of the center layer.

The difference between both the localization of the minority spin  $d$ -bands and the band narrowing of the majority spin  $d$ -bands of Fe( $S$ ) in the both terminations is consistent with a strong imbalance between the majority and minority  $d$ -electrons. Consequently, a larger enhancement of the magnetic moment of Fe( $S$ ) of the MgFe-Term (2.51  $\mu_B$ ) is induced in comparison with that of the CFe-Term (1.97  $\mu_B$ ).

It is found that the overall DOS shapes of Fe of the CFe-Term are similar to each other by comparing those from the subsurface to the center layers, while those of the MgFe-Term are similar to each other from the  $S$ -3 to the center layers. In the  $S$ -1 layer of the MgFe-Term, the DOS value of the majority spin bands of the Fe( $S$ -1) is increased at  $\sim$ -1.9 eV, but it is decreased at  $\sim$ -1.3 eV. The DOS peak around  $\sim$ -2.9 eV of the majority spin Fe( $S$ -1)- $d$  bands is broadened comparing to that of Fe( $C$ ). In the  $S$ -2 layer of the MgFe-Term, the peak of the majority spin  $d$ -bands of Fe( $S$ -2) at  $\sim$ -1.9 eV is increased much, the peak at  $\sim$ -1.5 eV is decreased slightly, and the peak at  $\sim$ -1.3 eV of the Fe( $C$ ) is shifted by -0.2 eV.

It is possible to understand all the above features by a simple symmetric point of view. In bulk MgCFe<sub>3</sub>, an Fe atom has two C atoms as the nearest-neighbors (n.n.), and has eight and four Fe and Mg atoms as the next-nearest-neighbors (n.n.n.), respectively. In the MgFe-Term, the Fe atom at surface loses one n.n. C and four n.n.n. Fe. On the other hand, in the CFe-Term, the Fe atom at surface loses only two n.n.n. Fe and Mg atoms, respectively. Therefore, the broken symmetry alters the electronic structures and magnetism of surface atoms of the MgFe-Term rather than that of the CFe-Term.

#### 4. Summary

We have investigated the electronic structures and magnetism of the non-oxide perovskite MgCFe<sub>3</sub>(001) surfaces in terms of the first-principles calculation by using the all-electron FLAPW method within the GGA. For comparison, we have considered two surface terminations, *i.e.* the MgFe-Term and the CFe-Term.

We found that the charge density profile of the CFe-Term is steeper than that of the MgFe-Term. The decrement of total  $p$ -electrons of the Fe( $S$ ) and the Mg( $S$ ) are 0.17 and 0.09 in the MgFe-term, which are much larger

than those of 0.05 of the Fe( $S$ ) and 0.02 of the C( $S$ ) in the CFe-Term. The increment (decrement) of the majority (minority)  $d$ -electrons of Fe( $S$ ) of the MgFe-Term are 0.46 (0.55) with respect to the center layer, which are larger than that of 0.21 (0.29) of the CFe-Term. The work functions are calculated to be 4.10 eV and 4.73 eV for the MgFe-Term and the CFe-Term, respectively. The spin density profile of the MgFe-Term is more erupted than that of the CFe-Term. This feature is consistent to the fact that the magnetic moment of Fe( $S$ ) of the MgFe-Term is increased by 1.06  $\mu_B$  from the center layer to 2.51  $\mu_B$ . From the spin-polarized layer-projected DOS, we found that the minority spin  $d$ -bands of Fe( $S$ ) of the MgFe-Term are strongly localized, while the localization of the minority Fe( $S$ )  $d$ -bands of the CFe-Term was suppressed much by the strong hybridization between the Fe- $d$  and C- $p$  states. The majority Fe( $S$ )  $d$ -bands of the MgFe-Term are narrower than those of the CFe-Term. These facts are consistent with the larger enhancement of magnetic moment of Fe( $S$ ) of the MgFe-Term with respect to that of the CFe-Term.

#### Acknowledgments

This work was supported by the Inha University Specialized Research Program (Next Generation Nano-Materials: INHA-21638).

#### References

- [1] T. He, Q. Huang, A. P. Ramirez, Y. Wang, K. A. Reran, N. Rogado, M. A. Hayward, M. K. Haas, J. S. Slusky, K. Inumara, H. W. Zandbergen, N. P. Ong, and R. J. Cava, *Nature* (London) **411**, 54 (2001).
- [2] J. H. Shim, S. K. Kwon, and B. I. Min, *Phys. Rev. B* **64**, 180510(R) (2001).
- [3] J. H. Shim, S. K. Kwon, and B. I. Min, *Cond-mat/0110448* (2001).
- [4] H. Rosner, R. Weht, M. D. Johannes, W. E. Pickett, and E. Tosatti, *Phys. Rev. Lett.* **88**, 027001 (2002).
- [5] Andrzej Szajek, *J. Phys.: Condens. Matter* **13**, L595-L600 (2001).
- [6] I. G. Kim, J. I. Lee, and A. J. Freeman, *Phys. Rev. B* **65**, 064525 (2002).
- [7] I. G. Kim, J. I. Lee, and A. J. Freeman, *Phys. Rev. B* **76**, 174512 (2002).
- [8] E. Wimmer, H. Krakauer, M. Weinert, and A. J. Freeman, *Phys. Rev. B* **24**, 864 (1981), and references therein; M. Weinert, E. Wimmer, and A. J. Freeman, *Phys. Rev. B* **26**, 4571 (1982).
- [9] J. P. Perdew and Y. Wang, *Phys. Rev. B* **45**, 13244 (1992).
- [10] D. D. Koelling and B. N. Harmon, *J. Phys. C* **5**, 1629 (1972).